



Dual-functional liposomes for curcumin delivery and accelerating silk fibroin hydrogel formation

Chavee Laomeephol^{a,b,f}, Helena Ferreira^{c,d}, Sorada Kanokpanont^{a,b,e}, Nuno M. Neves^{c,d}, Hisatoshi Kobayashi^{f,*}, Siriporn Damrongsakul^{a,b,e,*}

^a Biomedical Engineering Research Center, Faculty of Engineering, Chulalongkorn University, Bangkok 10330, Thailand

^b Biomaterial Engineering for Medical and Health Research Unit, Faculty of Engineering, Chulalongkorn University, Bangkok 10330, Thailand

^c 3B's Research Group, I3Bs - Research Institute on Biomaterials, Biodegradables and Biomimetics, University of Minho, Headquarters of the European Institute of Excellence on Tissue Engineering and Regenerative Medicine, AvePark - Parque de Ciência e Tecnologia, Zona Industrial da Gandra, 4805-017 Barco, Guimarães, Portugal

^d ICVS/3B's - PT Government Associate Laboratory, Braga/Guimarães, Portugal

^e Department of Chemical Engineering, Faculty of Engineering, Chulalongkorn University, Bangkok 10330, Thailand

^f International Center for Materials Nanoarchitectonics (WPI-MANA), National Institute for Materials Science (NIMS), Ibaraki, Japan

ARTICLE INFO

Keywords:
Silk fibroin
Curcumin
Liposome
Hydrogel
Anticancer

ABSTRACT

The administration of a drug-loaded implantable hydrogel at the tumor site after surgical resection is a viable approach to prevent the local recurrence or metastasis. Dimyristoyl glycerophosphorylglycerol (DMPG)-based liposomes were developed for inducing the rapid gelation of silk fibroin (SF) and delivering an anticancer drug, curcumin. Curcumin was loaded in the liposomes and the stability of curcumin was enhanced. The gelation time of liposome-induced SF hydrogels ranged from 3 min to more than 6 h. The biological activity of liposome-SF hydrogels was evaluated *in vitro* using L929 fibroblasts and MDA-MB-231 breast cancer cells. The release of curcumin can inhibit the growth of cancer cells. Both cells cultured on the surface of the hydrogels loaded with curcumin displayed low cell survival due to the combination of low cell attachment and cytotoxicity of curcumin. Liposome-SF hydrogels show potential as a sealant administered at the tumor site to eliminate residual cancer cells after tumor removal.

1. Introduction

Surgical resection is one of the recommended practices for the treatment of solid tumors, such as breast cancer (William et al., 2018). However, residual microtumors after operation could cause local recurrence or development of metastasis (Ceelen et al., 2014). Neoadjuvant chemotherapeutics or radiotherapy are, therefore, prescribed to eradicate the leftover cancer cells (William et al., 2018). However, some limitations exist, such as an inadequate drug accumulation at the tumor site, systemic toxicity, and low patient compliance (Qi et al., 2018). Local administration of chemotherapy can be an alternative to achieve higher local drug concentrations as well as to reduce systemic adverse effects (Wolinsky et al., 2012). Recently, local drug delivery is achieved by implantable formulations (e.g. hydrogels, micro/nanoparticles, films) based on biopolymers, due to their biocompatibility, biodegradability and capability to control the release of loaded therapeutic agents (Talebian et al., 2018; Wolinsky et al., 2012). An

injectable hydrogel with a thixotropic or an *in situ* gel forming characteristic, is a promising approach for the local treatment of tumors since drugs can be delivered in a confined space by using a minimally invasive administration (Talebian et al., 2018).

In this work, silk fibroin (SF), a protein obtained from *Bombyx mori* silkworm cocoons, was used for hydrogel fabrication due to its outstanding physicochemical and biological characteristics for tissue engineering and drug delivery applications. In addition to biodegradability and biocompatibility, SF possesses an excellent mechanical strength compared to other natural biomaterials, leading to its widely use in tissue engineering of load-bearing tissues, e.g. bone and cartilage, as well as other tissues requiring high mechanical stability, such as skin, cardiac muscle, and blood vessel (Bhattacharjee et al., 2017; Kundu et al., 2013). Versatility in fabrication of SF into various frameworks, namely films, fibers, scaffolds, particles, and hydrogels, allows its design to match the specific requirements of the different applications. In a drug delivery field, the geometry in combination with inherent

* Corresponding authors at: Biomedical Engineering Research Center, Faculty of Engineering, Chulalongkorn University, Bangkok 10330, Thailand (S. Damrongsakku).

E-mail addresses: kobayashi.hisatoshi@nims.go.jp (H. Kobayashi), siriporn.d@chula.ac.th (S. Damrongsakku).

<https://doi.org/10.1016/j.ijpharm.2020.119844>

Received 8 May 2020; Received in revised form 14 August 2020; Accepted 31 August 2020

Available online 06 September 2020

0378-5173/ © 2020 Elsevier B.V. All rights reserved.

Table 1
Different formulations of liposomes.

DMPG:DMPC:Chol:Cur weight ratio	Code	DMPG (mg)	DMPC (mg)	Chol (mg)	Cur (mg)
10:0:0:0.5	A0	50	0	0	2.5
7:3:0:0.5	B0	35	15	0	2.5
5:5:0:0.5	C0	25	25	0	2.5
3:7:0:0.5	D0	15	35	0	2.5
10:0:1:0.5	A1	50	0	5	2.5
7:3:1:0.5	B1	35	15	5	2.5
5:5:1:0.5	C1	25	25	5	2.5
3:7:1:0.5	D1	15	35	5	2.5
10:0:2:0.5	A2	50	0	10	2.5
7:3:2:0.5	B2	35	15	10	2.5
5:5:2:0.5	C2	25	25	10	2.5
3:7:2:0.5	D2	15	35	10	2.5

properties of the biomaterials affect the drug release mechanisms. SF has been used to control the release and preserve the bioactivities of entrapped substances, e.g. genes, small molecule, and biological drugs, throughout the duration of release (Yucel et al., 2014).

Self-assembly of SF in solution allows the formation of a gel due to the spontaneous transformation of predominated random coil structure to the highly stable beta sheet (Matsumoto et al., 2006). This process can be accelerated to achieve the complete gelation within minutes or hours using several physical interventions or chemical additives. Furthermore, the lack of cell-binding affinity in the primary structure of SF (Zhou et al., 2001) can decrease cell affinity and delay cell adhesion and proliferation (Acharya et al., 2008; Amornsudthiwat et al., 2013). These properties make SF a suitable matrix for the application as a sealant used after tumor removal.

Derived from *Curcuma longa*, curcumin has been well known as a multipurpose medicine due to its anti-inflammatory, antioxidant and anti-cancer activities (Mehanny et al., 2016). Molecular targets of curcumin relating to an inhibition of tumor initiation and progression include the suppression of NF- κ B and tumor necrosis factor (TNF) expression, a down-regulation of cyclin D, and an activation of caspase families (Mehanny et al., 2016; Shishodia et al., 2007). However, crucial limitations of using curcumin as a medicine include its low aqueous solubility and rapid degradation (Mehanny et al., 2016; Wang et al., 1997).

Nanotechnology in the drug delivery field improves the pharmacological outcomes of the loaded bioactive substances by enhancing pharmacokinetics, improving drug loading and stability, and providing specific targeting (Patra et al., 2018). Liposomes are one of the most applied nanostructures for entrapping drug molecules since their membrane structures allow the encapsulation of both hydrophilic and hydrophobic drugs. Hence, liposomes can be utilized to entrap curcumin to increase curcumin solubility and prevent the degradation from hydrolysis and photo-induced reaction in the biological milieu (Mehanny et al., 2016).

However, the administration of nanocarriers, which are typically in suspension, might not be suitable for local administration due to fast dissipation from injection site and non-sustained drug release. Hydrogel loaded with nanocarriers, such as liposomes, were introduced to control the release as well as to accumulate the drug at the target site (Grijalvo et al., 2016; Pitorre et al., 2017). Our previous study reported that a negative-charged phospholipid, 1,2-dimyristoyl-*sn*-glycero-3-phospho-*rac*-(1-glycerol) sodium salt (DMPG), can accelerate the SF gelation to 10–40 min depending on the concentration of DMPG (Laomeephol et al., 2020). Mechanisms of DMPG in accelerating SF gelation were investigated and the obtained hydrogels were used for cell encapsulation. Also, DMPG can be a component for the preparation of liposomes (Li et al., 2015), which were used for the entrapment of lipophilic molecules in combination with a zwitterionic phospholipid, 1,2-dimyristoyl-*sn*-glycero-3-phosphocholine (DMPC) (Han et al., 2002; Sampedro et al., 1994). Therefore, DMPG-based liposomes were

prepared to function as a delivery system of curcumin and an inducer of SF gelation. Liposomes with varied phospholipid (DMPG:DMPC) and cholesterol ratio were prepared and their characteristics, including production yield, size, and morphology, were determined. Moreover, the entrapment efficiency of curcumin in different liposome formulations to increase drug solubility and stability was investigated. The gelation of liposome and SF mixtures was also evaluated. The release profile of curcumin from the hydrogels and its biological activities were assessed for the feasibility of the developed hydrogel as a sealant administered after tumor resection.

2. Materials and methods

2.1. Materials

Thai domesticated *Bombyx mori* silkworm cocoons were supplied from Queen Sirikit Sericulture Center, Srisaket province, Thailand. Phospholipids, 1,2-dimyristoyl-*sn*-glycero-3-phospho-(1'-*rac*-glycerol) sodium salt (DMPG) and 1,2-dimyristoyl-*sn*-glycero-3-phosphocholine (DMPC), were purchased from Lipoid GmbH, Germany. Curcumin (Cur) was acquired from Sigma-Aldrich, USA. All chemicals were of analytical grade and supplied from Wako Chemicals, Japan. Culture media and reagents for biological assays were obtained from Thermo Fischer Scientific, USA unless otherwise stated.

2.2. Liposomes preparation

Liposomes were prepared using the lipid film hydration method followed by bath sonication. Firstly, the mixtures of DMPG, DMPC, cholesterol (Chol) and Cur at different ratios (Table 1) were placed in round bottom flasks. The organic solvents were eliminated by a rotary evaporator (N-1100, Eyela, Japan) using a pressure and bath temperature fixed at 50 mbar and 40 °C, respectively. After that, distilled water was added, and the mixtures were vortexed before bath sonication at 40 °C for 1 h with occasional shaking. The obtained liposomes were centrifuged at 4 °C for 10 min and filtered through 0.22- μ m filter to remove precipitated Cur.

2.3. Liposomes characterization

2.3.1. Liposomes yield and Cur content assessment

Yield percentage was calculated based on the dry solid weight of liposomes compared to their initial weight. Amount of Cur entrapped in the liposomes was determined by a spectrophotometric method. To do this, the liposomes were mixed in ethanol at 2.5% vol to disrupt the structure and dissolve Cur. The absorbance of the ethanolic solutions at 415 nm was collected using a microplate reader (MTP-880Lab, Corona Electric, Japan). Loading capacity (LD) and encapsulation efficiency (EE) were calculated using the following equations:

$$\%LD = \frac{Cur_{abs}}{W_{lip}} \times 100$$

$$\%EE = \frac{Cur_{abs}}{Cur_{cal}} \times 100$$

where Cur_{abs} is the amount of Cur in mg calculated from the absorbance value, W_{lip} is the solid weight of liposomes after preparation, and Cur_{cal} is the theoretical amount of Cur calculated based on the W_{lip} .

2.3.2. Size distribution and microstructure of liposomes

Size and polydispersity index (PDI) of liposomes were measured by light scattering using a dynamic light scattering photometer (DLS-8000HAL, Otsuka Electronics, Japan) equipped with a 488-nm laser.

The morphological features of liposomes were observed using a transmission electron microscope (TEM) and a negative staining technique. The liposome samples (A1, B1, C1, and D1; 0.5 mg/mL) were filtered through a membrane filter (0.22- μ m pore size) prior to staining procedure. The samples were dropped onto a high resolution carbon film copper grip (HRC-10, Okenshoji, Japan), and, after 2 min, the excess was blotted away with a filter paper. Then, a drop of 2% phosphotungstic acid (pH 7) was added. After 2 min, the excess of the solution was removed. The grid was left to dry prior to TEM observation (JEM-2100, Jeol, Japan).

2.3.3. Analysis of active curcuminoids in Cur by liquid chromatography/mass spectrometry (LC/MS)

LC/MS was used to determine biological active curcuminoids in Cur, namely curcumin, demethoxycurcumin (DMC), and bisdemethoxycurcumin (BDM), following the method reported by Ramalingam *et al* (Ramalingam and Ko, 2014) and Yang *et al* (Yang *et al.*, 2007) with slight modifications. The liposomes were dissolved in ethanol at 2.5% vol, before injecting to a liquid chromatography system (Prominence LC-20AD, Shimadzu, Japan). The chromatographic separation was achieved using an InertSustain™ reverse phase C18 column (150 \times 4.6 mm I.D., 5 μ m; GL Sciences, Japan). A mobile phase containing 70:30 acetonitrile:0.1% v/v formic acid was used, and the flow rate was fixed at 400 μ L/min. The temperature of the autosampler and column was maintained at 4 and 40 °C, respectively. The run time was 10 min and the spectral profile was collected by a photodiode array (PDA; Prominence SPD-M20A, Shimadzu, Japan) detector.

The identification of curcuminoids was conducted using a MS/MS system (LXQ, Thermo Scientific, USA) under a negative mode. The electrospray ionization (ESI) parameters were set as following: 25 eV for capillary voltage and 320 °C for the desolvation temperature. Multiple reaction monitoring (MRM) mode was used to monitor the ionization transition of analytes, being of 368 > 217 *m/z* for curcumin, 338 > 217 *m/z* for DMC, and 308 > 187 *m/z* for BDM. Chemical structures of curcuminoids and mass spectral profile are shown in Fig. 1A, and the spectra of ionized products of curcumin, DMC and BDM are presented in Fig. 1B, C and D, respectively.

2.4. Liposome-induced SF hydrogels

2.4.1. Preparation of SF solution

SF solution was prepared following the method reported previously (Vachiraroj *et al.*, 2009). Briefly, silk cocoons were boiled in 0.2 M Na₂CO₃ to eliminate silk sericin and to obtain the SF fibers. The fibers were then dissolved in 9.3 M LiBr at 60 °C for 4 h before dialysis against deionized water for 48 h using a semi-permeable membrane with molecular weight cut-off of 12–16 kDa (Sekisui, Japan). The concentration of the regenerated SF solution was determined from its dry solid weight.

2.4.2. Gelation time

SF solution was mixed with liposomes to a final concentration of 3% SF and 10 mg/mL liposomes (equivalent to 15 mM phospholipids). The

gelation of liposome-SF mixtures was determined from the turbidity changes by collecting absorbance values at 540 nm every minute for 6 h using a microplate reader (iMark™, Bio-rad, USA). Gelation time was analyzed from the point at which the absorbance reaches the half-maximum values.

2.4.3. Microstructural analysis

The liposome-SF mixtures, prepared as described in the Section 2.4.2, were incubated for 24 h at 37 °C to allow the formation of the hydrogels. Regenerated SF and Cur-loaded SF (Cur-SF) hydrogels were prepared by sonication method according to Wang *et al.* (2008). 3% SF solution and the solution with 0.5 mg/mL Cur were sonicated using a probe sonicator (Vibra-Cell VCX130, Sonics&Materials, Inc., USA) at 50% amplitude for 1 min and the hydrogels were obtained within 1 h. All hydrogels were frozen at –20 °C overnight and lyophilized for 48 h. Microstructural features of the freeze-dried samples were analyzed by a scanning electron microscope (SEM; Miniscope TM3000, Hitachi High-Technologies, Japan) without coating. The elemental analysis was conducted using an equipped energy-dispersive x-ray spectroscopy (EDX).

TEM analysis was conducted to characterize the microstructure of the liposome-SF hydrogels. The mixtures of 0.075% SF solution and 0.5 mg/mL liposomes (A1, B1, C1, and D1) were prepared and filtered before adding to the TEM grids. The negative staining and TEM imaging were conducted as previously mentioned.

2.4.4. Unconfined mechanical testing

The compressive mechanical properties of the hydrogels were analyzed using a texture analyzer (TA-XT2i, Hidehiro, Japan) equipped with 1 kN load cell. Cylindrical-shape SF, Cur-SF and liposome-SF hydrogels measuring 5 mm in diameter and 2 mm in height were kept in the phosphate buffer saline (PBS) at 37 °C until the measurement. The hydrogels were prepared using the autoclaved SF solution and filtered Cur in dimethyl sulfoxide (DMSO) or liposomes to mimic the properties of the hydrogels used for *in vitro* biological experiments. The samples were compressed by a 5-mm diameter probe displaced at a controlled speed of 0.1 mm/sec. The results from at least 15 samples were collected to ensure the reliability. The elastic modulus was determined from the slope of the stress–strain plot in the linear elastic region.

2.4.5. Cur release

Regenerated SF, Cur-SF and liposome-SF hydrogels were punched into a disc shape with 2-mm thickness and 5-mm diameter and placed in 1 mL of release media (PBS, pH 7.4 + 10% fetal bovine serum (FBS) + 0.01% sodium azide). At each time point, 100 μ L of supernatant was collected and replaced with a same amount of release buffer. The absorbance values at 415 nm were measured and the amount of released Cur was calculated using a standard curve. All materials were sterilized, and the experiments were done under aseptic conditions to avoid contamination.

2.5. Biological evaluation

2.5.1. Cell culture

A mouse lung fibroblast cell line, L929, and human breast cancer cells, MDA-MB-231, were selected to evaluate the cytotoxicity and the biological activity of liposome-SF hydrogels. L929 was maintained in Dulbecco's Modified Eagle Medium (DMEM)-high glucose supplemented with 10% FBS and 1% antibiotics. MDA-MB-231 was cultured in DMEM-high glucose with 10% FBS, 1% antibiotics, non-essential amino acid, and 1 mM sodium pyruvate. All cells were cultured at 37 °C in humidified air supplemented with 5% CO₂. Subculture was performed when the cell confluency achieved approximately 80–90% using trypsin solution for cell detachment.

To prepare the hydrogels for cell culture, SF solution was sterilized by autoclaving at 121 °C, 20 min, and liposomes were filtered through

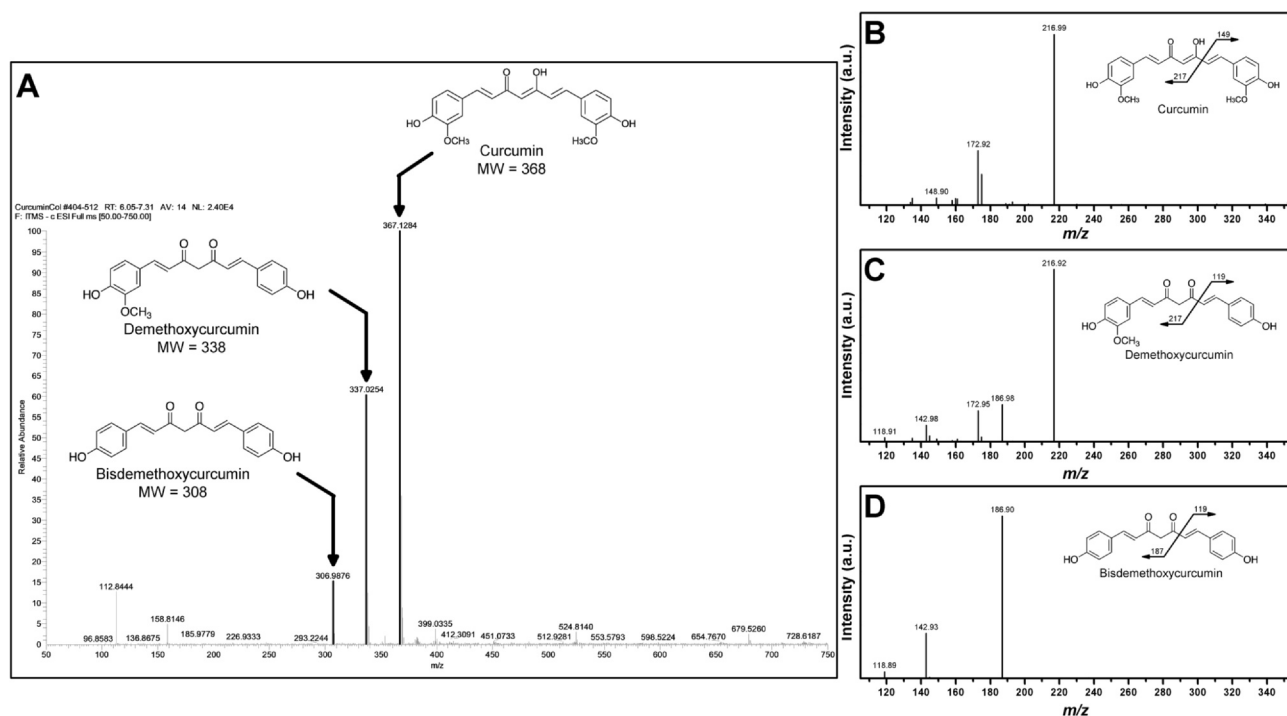


Fig. 1. LC/MS analysis of standard Cur in ethanol: (A) Full scan mass spectrum of curcumin, DMC, and BDM, indicating the molecular mass of 367.13, 337.03 and 306.99, respectively. Secondary mass spectra and the fragmentation transition of ionized (B) curcumin ($368 > 217\ m/z$), (C) DMC ($338 > 217\ m/z$), and (D) BDM ($308 > 187\ m/z$).

0.22- μm filter. All hydrogels were prepared as previously described under aseptic conditions.

The cytotoxicity of Cur released from the hydrogels to L929 or MDA-MB-231 was evaluated. Cells were firstly plated at a density of 10,000 cells/ cm^2 . After 6 h (to allow the complete attachment of cells), the hydrogels in a disc shape (5-mm diameter and 2-mm thickness) were put into each well with 1 mL cell culture medium. The viability of the cells cultured on the surface of the hydrogels was evaluated by seeding the cells (20,000 cell/ cm^2) on hydrogels placed in each well of 48-well plates. All plates were kept in CO_2 incubator at 37 $^\circ\text{C}$. Media were changed every other day. For both experiments, cells cultured on tissue culture plate (TCP) were used as control.

2.5.2. Cell viability

Cell viability at each time point (1, 3, 5 and 7 days) was determined using WST-1 cell metabolic activity assay (Takara Bio, Japan) following the manufacturer's instruction. In brief, cells were washed with PBS once before adding 300 μL of WST-1 solution. The samples were incubated at 37 $^\circ\text{C}$ for 2 h in the dark, and the absorbance values of supernatants were measured at 450 nm with a reference filter at 570 nm.

2.5.3. Cell apoptosis staining and cell imaging

After cultured for 1 day, cells were stained with fluorescein-annexin V and 7-aminoactinomycin D (7-AAD; Sony Biotechnology, USA) to detect cell apoptosis according to the manufacturer's instruction. Briefly, cells were washed with PBS once before staining with the solutions of fluorescein-annexin V and 7-AAD, and incubated for 15 min. The stained cells were visualized using a fluorescence microscope (IX71, Olympus Lifescience, Japan). Fluorescence intensity of the annexin V and 7-AAD stained cells images were analyzed using ImageJ software. Original fluorescence images were converted to 8-bit grayscale images, and average fluorescence intensities of labelled cells were measured.

2.6. Statistical analysis

Statistical analysis was performed using one-way analysis of variance (ANOVA) followed by Bonferroni post hoc test at $p \leq 0.05$. The difference of the data from different samples within the same time point was analyzed. IBM SPSS Statistics 22 software was used to perform statistical tests.

3. Results

3.1. Liposomes characterization and Cur content assessment

To investigate an optimum liposome formulation using DMPG as a based phospholipid to entrap Cur, the liposomes prepared from DMPG or different ratios of DMPG and DMPC as well as different added content of Chol were fabricated. The liposome characteristics, including yield, entrapped Cur content and size of liposomes were analyzed from 4 batches and the results are presented in Table 2. Gravimetric method was used to determine the preparation yield and the result showed that approximately 80–90% yield was obtained. To evaluate the entrapped Cur, the liposome structure was disrupted by dissolving in ethanol, and the amount of Cur was measured spectrophotometrically. The EE ranged from 50 to 100% depending on the formulations tested while 1–5% LD was achieved. The liposomes with higher cholesterol ratio showed lower EE and LD. Size of liposomes, determined by DLS technique, was in the range of 100 to 300 nm. The higher ratio of DMPG to DMPC resulted in a broad size distribution, as found in A0 and B0. It can be noticed that the size of liposomes C and D was less scattered. Moreover, taking A1, B1, A2, and B2 as examples, the addition of Chol resulted in a more controllable liposome size.

To evaluate the stability of the obtained liposomes, they were kept at 4 $^\circ\text{C}$ for 2 weeks before repeating the size analysis. No significant changes were observed for all liposome formulations except the noticeable broad size distribution of A0 and B0 (Fig. 2).

Fig. 3 shows TEM images of liposomes A1, B1, C1 and D1. The round morphology can be noticed as well as the unilamellar structure.

Table 2

Yield of production, encapsulation efficiency (EE) and loading capacity (LD) of Cur, size, and polydispersity index (PDI) of the liposomes.

Liposomes	Yield (%)	EE (%)	LD (%)	Size (nm)	PDI
A0	94.60 ± 8.34	69.82 ± 19.09	3.33 ± 0.91	1054.74 ± 2085.78	0.3609 ± 0.1472
B0	81.27 ± 10.60	105.14 ± 11.74	5.01 ± 0.56	298.89 ± 574.85	0.2154 ± 0.2403
C0	81.90 ± 16.67	97.68 ± 14.31	4.65 ± 0.68	104.61 ± 8.28	0.2392 ± 0.0519
D0	78.10 ± 19.85	102.67 ± 9.34	4.88 ± 0.44	135.07 ± 10.24	0.2282 ± 0.0397
A1	88.84 ± 14.81	52.01 ± 11.50	2.26 ± 0.50	160.18 ± 73.14	0.1981 ± 0.0516
B1	85.22 ± 18.21	62.77 ± 17.76	2.73 ± 0.77	160.79 ± 50.91	0.2037 ± 0.0650
C1	89.57 ± 13.17	65.49 ± 23.46	2.85 ± 1.02	111.83 ± 19.36	0.2122 ± 0.0346
D1	84.64 ± 13.06	94.06 ± 17.99	4.09 ± 0.78	167.50 ± 23.41	0.2258 ± 0.0307
A2	84.80 ± 11.95	39.65 ± 7.72	1.59 ± 0.31	134.50 ± 32.75	0.2161 ± 0.0726
B2	79.73 ± 8.97	51.92 ± 15.27	2.08 ± 0.61	181.84 ± 26.60	0.2244 ± 0.0175
C2	75.47 ± 15.34	52.37 ± 9.81	2.10 ± 0.39	152.91 ± 29.94	0.2306 ± 0.0303
D2	83.20 ± 10.07	66.36 ± 22.66	2.65 ± 0.91	274.54 ± 50.49	0.2201 ± 0.0304

Irregular shapes are presented in the liposomes with higher DMPG ratio, i.e. A1 and B1. Furthermore, the size of single A1 and B1 liposomes (Fig. 3A and B) was smaller than the results determined by DLS. Presumably, the irregular shape and the aggregation of these liposomes resulted in the larger size and the broad size distribution.

3.2. LC/MS analysis of curcuminoids

Curcuminoid represents bioactive compounds in Cur extracts obtained from Turmeric composing of curcumin and its derivatives, DMC, and BDM. The lack of one or two methoxy groups linked to the phenol ring, respectively, results in different chemical properties, which can be distinguished by chromatographic separation. The chromatograms of a standard of Cur in ethanol are exemplified in Fig. 4. Three peaks at the retention time of 6.2, 6.5 and 6.9 min (Fig. 4A) with respective mass of 307.02, 337.09, and 367.08 (Fig. 4B) were noticed, indicating the characteristic peaks of BDM, DMC, and curcumin, respectively. The results were in accordance with the previous report (Yang et al., 2007). The amount of curcuminoids can be determined from the area under its corresponding peak of PDA spectra.

Fig. 4C presents the amount of curcuminoids determined from LC/MS normalized by the amount from spectrophotometric assay of entrapped Cur in liposomes. Approximately 30–50% of active curcuminoids were noticed in the liposomes, and the amount of curcuminoids was relatively lower for a higher cholesterol ratio. The stability of entrapped curcuminoids in the liposomes stored at 4 °C for 2 weeks was also evaluated. The results showed no or slight difference between the freshly prepared liposomes and the 2-week stored liposomes.

To determine the aqueous solubility and stability of Cur without liposomal encapsulation, 200 µg/mL Cur directly dissolved in water was prepared and the solution was analyzed accordingly. An amount of 0.54 µg/mL curcuminoids was detected, confirming the low aqueous solubility of Cur. Moreover, after the solution stored at 4 °C for 2 weeks, only 0.05 µg/mL curcuminoids were quantified. The results confirm

that the encapsulation of Cur in liposomes enhances their amount as well as the stability of active curcuminoids.

3.3. Gelation time of liposome-SF hydrogels

As previously mentioned, the gelation of regenerated SF solution without any intervention spontaneously occurred due to self-assembly, but the gelation time was very long. The DMPG-based liposomes were developed to enhance Cur loading as well as intrigue the rapid gelation of SF solution. The liposomes were simply added to SF solution and the gelation kinetic was followed from the turbidity change. The gelation time of liposome-SF mixtures presented in Table 3 indicates that the addition of Chol extended the gelation time of SF. Moreover, the decreasing of DMPG ratio, from DMPG:DMPC 10:0 to 3:7, resulted in a longer gelation time. The gelation of SF did not occur within 6 h upon a presence of liposome D (DMPG:DMPC, 3:7). These results were in accordance with our previous study (Laomeephol et al., 2020). However, the gelation of D0-SF and D1-SF occurred after overnight incubation, but no gelation was observed for D2-SF.

3.4. SEM and TEM analysis of liposome-SF hydrogels

The porous microstructures with leaf-like wall can be visualized in all freeze-dried samples with a comparable pore size of 100–200 µm (Fig. 5). Noticeably, small distributed particles can be noticed in Cur-SF hydrogels, while cannot be observed in other samples. The elemental analysis of the liposome-SF hydrogels indicated the presence of Na and P, the elements presenting in DMPG and DMPC.

The TEM images of liposomes A1-, B1-, C1- and D1-SF hydrogels are presented in Fig. 6. The liposomes were mixed with SF solution before coating on TEM grids, and the negative staining was performed. A large number of small vesicles with a size smaller than 50 nm were observed for A1-SF (Fig. 6A). The noticed size of liposomes in hydrogels was smaller than those of neat liposomes (Fig. 3A). However, the TEM

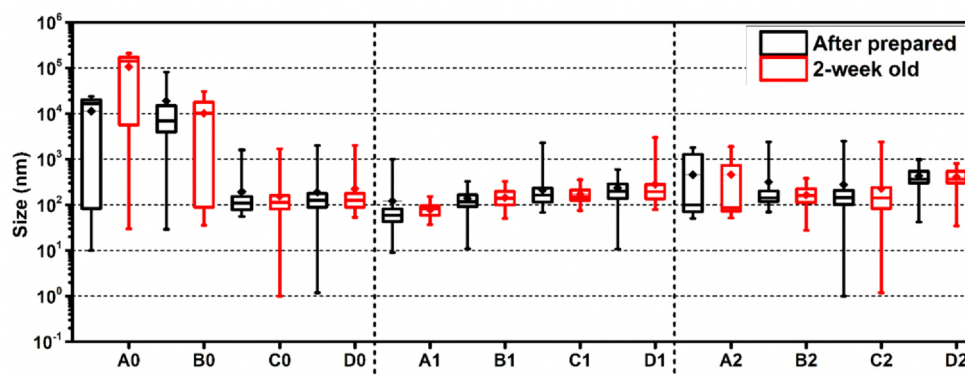


Fig. 2. Size of liposomes determined by DLS before (black box) and after 2-week storage at 4 °C (red box).

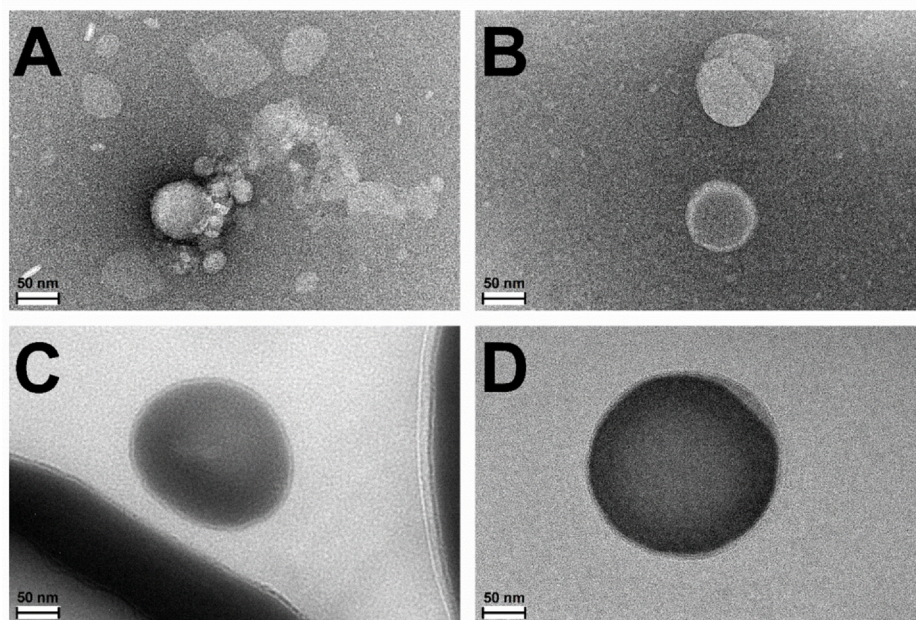


Fig. 3. TEM images of liposomes (A) A1, (B) B1, (C) C1 and (D) D1 (scale bar = 50 nm). The liposomes were coated onto TEM grids and stained by phosphotungstic acid (pH 7), before visualizing at an acceleration voltage of 200 kV.

images of the other hydrogels show that most liposomes remained in similar size and shape compared to the neat liposomes. The nanofibrous structure of SF was visible for all samples.

3.5. Mechanical properties of hydrogels

Elastic modulus, yield stress, and strain of the hydrogels assessed by the unconfined compression tests are present in Table 4. The hydrogels were immersed in PBS, and the measurement was conducted in the fully hydrated state. The significant lower elastic moduli than those of the regenerated SF hydrogels were noticed for Cur-loaded and liposome-loaded SF hydrogels. Higher yield stress and strain were noticed in the A1-SF and B1-SF hydrogels than those of the regenerated SF, Cur-SF, C1- and D1-SF hydrogels. From stress-strain plots of A1-SF and B1-SF hydrogels (Fig. 7), the materials possessed linear elasticity up to

Table 3

Gelation time (mean ± SD) of the mixtures of 3% SF and 10 mg/mL liposomes A, B, C and D with different Chol ratio. * indicates no gel formation within 6 h.

Liposomes	Gelation time (min)		
	Chol 0	Chol 1	Chol 2
A	3.4 ± 0.7	7.3 ± 2.0	18.9 ± 6.5
B	14.2 ± 4.0	22.0 ± 8.3	167.8 ± 34.0
C	79.6 ± 32.7	145.4 ± 49.8	–*
D	*	–*	–*

approximately 47–50% strain, before reaching the abrupt decreasing of stress. While the lower yield strains of other samples (regenerated SF, Cur-SF, C1-, and D1-SF hydrogels), at about 28–31%, and a constant

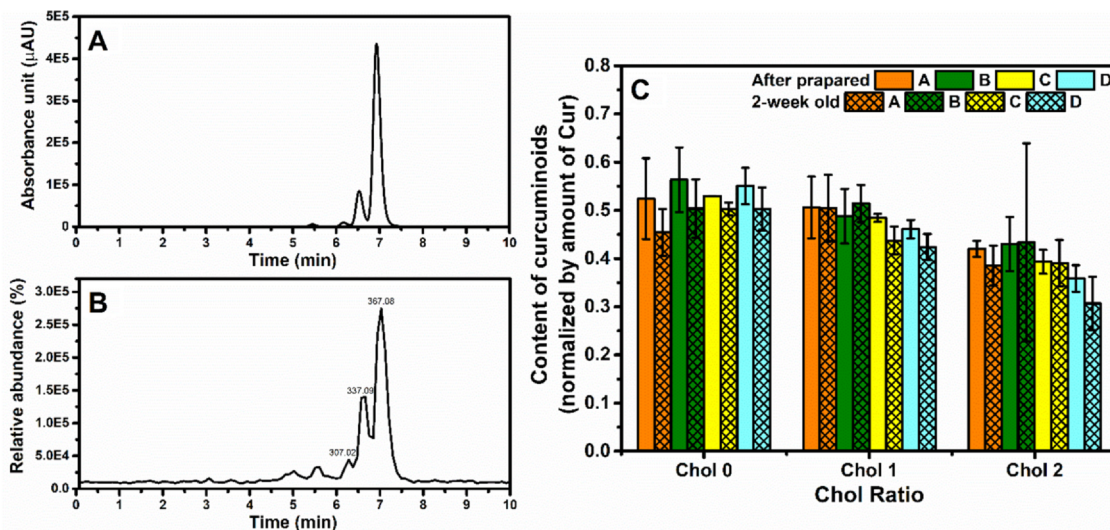


Fig. 4. LC/MS analysis of a standard Cur in ethanol: (A) PDA and (B) MS spectra. Three peaks at the retention of 6.2, 6.5 and 6.9 min, corresponding to the molecular mass of 307.02 (BDM), 337.09 (DMC), and 367.08 (curcumin), respectively. (C) Curcuminoid content of the freshly prepared (clear column) and 2-week stored liposomes (patterned column) calculated from the area under curve of LC/MS spectra and normalized by the amount of Cur obtained from the spectrophotometric assay.

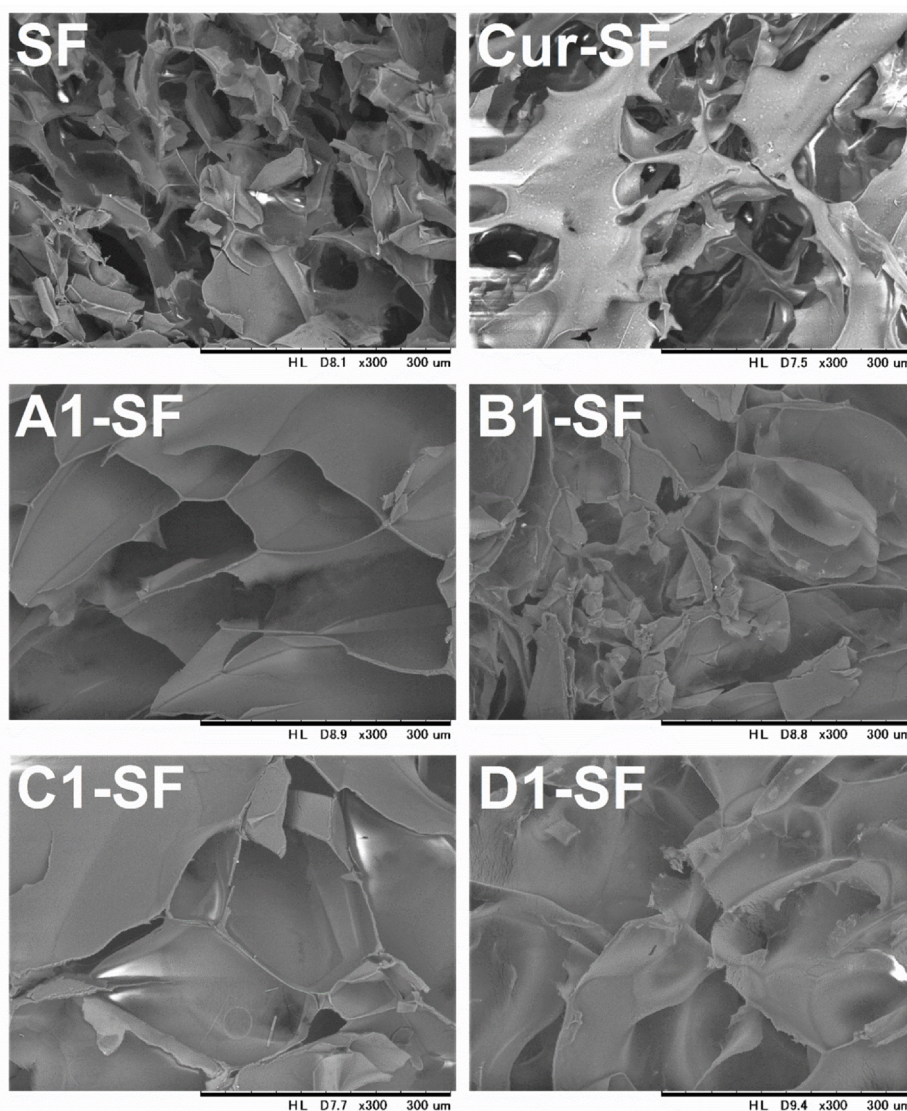


Fig. 5. SEM images freeze-dried SF, Cur-SF, and liposome (A1, B1, C1, D1)-SF hydrogels. Scale bar of SEM images is 300 μ m.

stress over a range of strain after the elastic limit were noticed.

3.6. Release of Cur from liposome-SF hydrogels

The release of Cur from sonicated Cur-SF hydrogels and liposome-induced SF hydrogels was evaluated. PBS supplemented with FBS was used as the release media to mimic the ionic conditions as well as the proteins presented in cell culture media. From 7-day release experiment, a burst release was noticed from all samples within the initial period of 24 h, before a gradual release into the media over the experimental time. Comparing the maximum release content of Cur from the different hydrogels, the following order can be established: Cur-SF \sim D1 > C1 > B1 \sim A1 (Fig. 8A). Approximately 20 to 35% of entrapped Cur was released from the hydrogels in 7 days. No significant difference was observed in the percentage of Cur release percentage, with an exception of the C1-SF hydrogel, which provided the lowest drug release (Fig. 8B).

3.7. Cell viability

As our main aim was to implement the hydrogels as a filler administered after tumor resection, L929 was selected as a representative of fibroblasts, which are recruited in an early phase of wound repair to

facilitate matrix production (Gailit and Clark, 1994), and MDA-MB-231 was selected as a cancer cell type. Fig. 9A and 9B show the viability of L929 and MDA-MB-231, respectively, plated on cell culture plates and exposed to Cur released from the samples immersed in the culture media. For L929, the lower cell activity was noticed in day 3 for all Cur-loaded hydrogel groups. However, when cultured for a longer period, the cells showed comparable activities to those of blank (TCP) and SF hydrogel groups. Significant differences were observed for MDA-MB-231. These cells showed a significant low cell activity when cultured with C1- and D1-SF hydrogels, comparing to SF hydrogels. The lowest cell viability of the positive control group (Cur-SF hydrogel) was noticed.

The viability and proliferation of cells in contact to the hydrogels were evaluated. The cells were cultured on the hydrogels and their viability was determined using the WST-1 cell metabolic assay. The results were collected at day 1, 3, 5, and 7, and presented in Fig. 9C and D. Compared to TCP group, the proliferation of cells on SF gels was substantially lower. However, the metabolic activity of cells on SF gradually increased over the culture period, indicating no cytotoxicity of SF. For Cur-SF and liposome-SF hydrogels, the metabolic activities of L929 and MDA-MB-231 were extremely low. Presumably, the SF substrate combining with released Cur could inhibit the proliferation of adjacent cells.

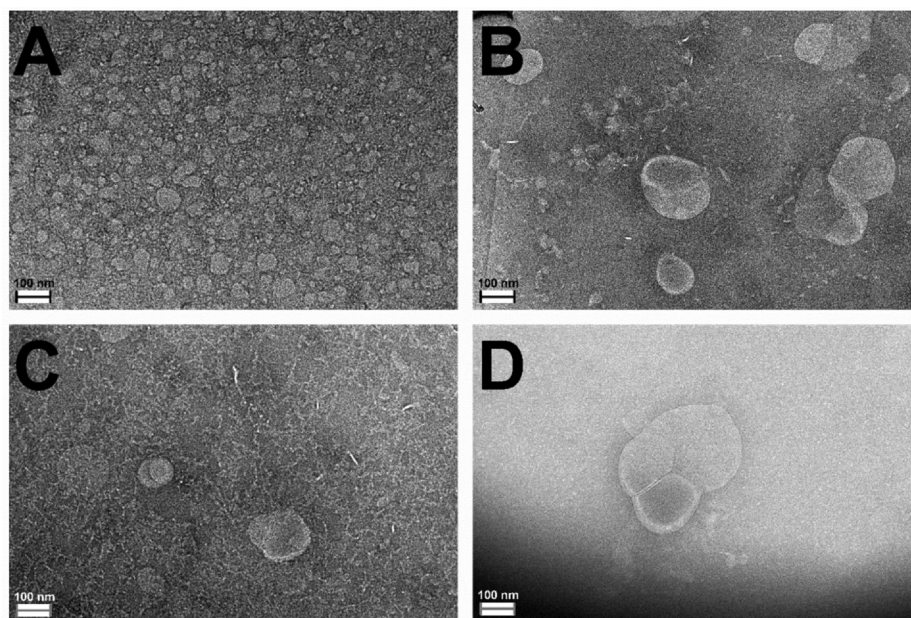


Fig. 6. TEM images of liposome-SF hydrogels (A) A1-SF, (B) B1-SF, (C) C1-SF and (D) D1-SF (scale bar = 100 nm). The liposomes were mixed with SF solution before coating on TEM grids and stained. The acceleration voltage of 200 kV was applied.

Table 4

Mechanical properties of the regenerated 3% SF, Cur-SF and liposome-SF hydrogels. The alphabets indicate the statistical difference at $p \leq 0.05$, compared to those of the SF hydrogels.

Hydrogels	Elastic modulus (kPa)	Yield stress (kPa)	Yield strain (%)
SF	0.84 ± 0.12^a	17.27 ± 1.65^c	30.87 ± 5.69^g
Cur-SF	0.67 ± 0.07^b	14.39 ± 1.52^d	28.56 ± 4.14^g
A1-SF	0.50 ± 0.06^c	22.86 ± 2.74^e	49.90 ± 4.70^h
B1-SF	0.67 ± 0.10^b	26.19 ± 2.58^f	47.35 ± 4.72^h
C1-SF	0.69 ± 0.17^b	12.53 ± 2.50^d	27.71 ± 5.89^g
D1-SF	0.72 ± 0.12^b	$16.40 \pm 2.88^{c,d}$	30.47 ± 5.59^g

3.8. Apoptosis staining of cells exposed to Cur released from hydrogels

Due to the auto-fluorescence of Cur, cells cultured on the surface of hydrogels and stained with fluorescent dyes cannot be observed. Therefore, only cells plated on TCP and cultured for 1 day in the media with hydrogels were stained with annexin V and 7-AAD. Then, their fluorescent images were collected to determine the apoptotic activities, and the fluorescence intensity of the stained fluorescent dyes were quantitatively analyzed. Cells stained by both annexin V and 7-AAD are in a late apoptosis or cell necrosis, while cells in an early apoptosis are positively stained with annexin V and not stained by 7-AAD. Fig. 10A and B show the fluorescence images of the stained L929 cells with their bright field images, and the quantitative analysis results of the

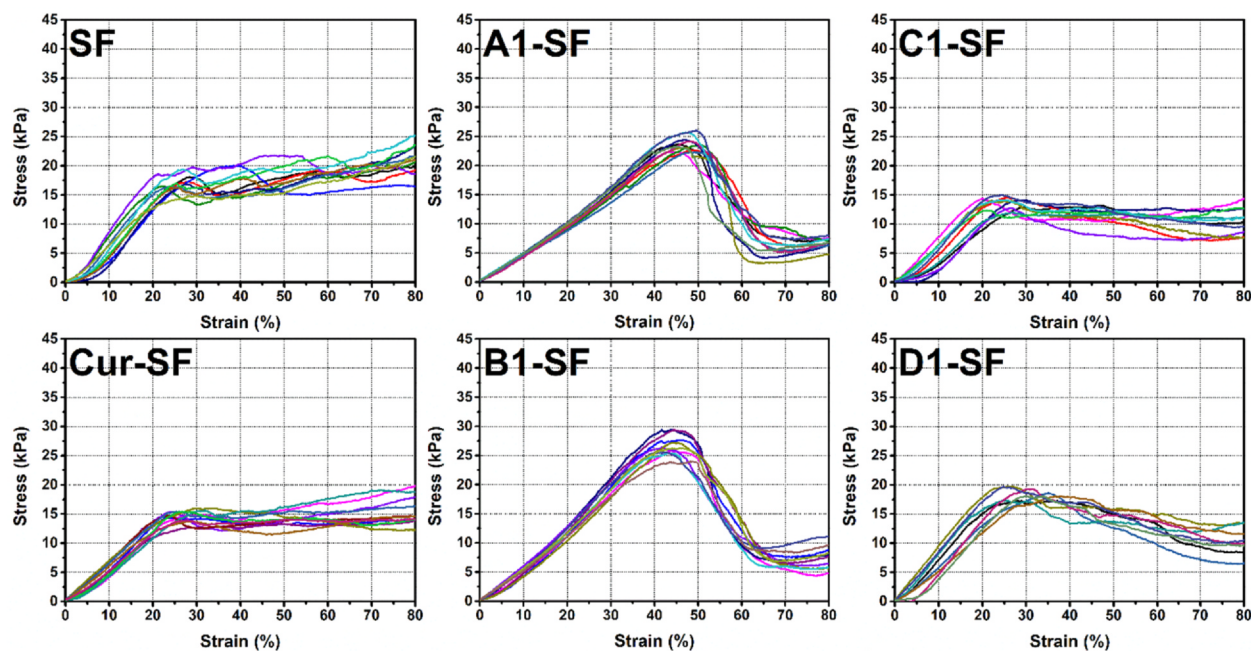


Fig. 7. Stress-strain plots of the regenerated SF, Cur-SF, and liposome-SF hydrogels assessed by the unconfined compression tests. The samples in disc shape with 5-mm diameter and 2-mm thickness were immersed in PBS buffer for 24 h prior to mechanical analysis. Each line represents the data obtained from each tested sample.

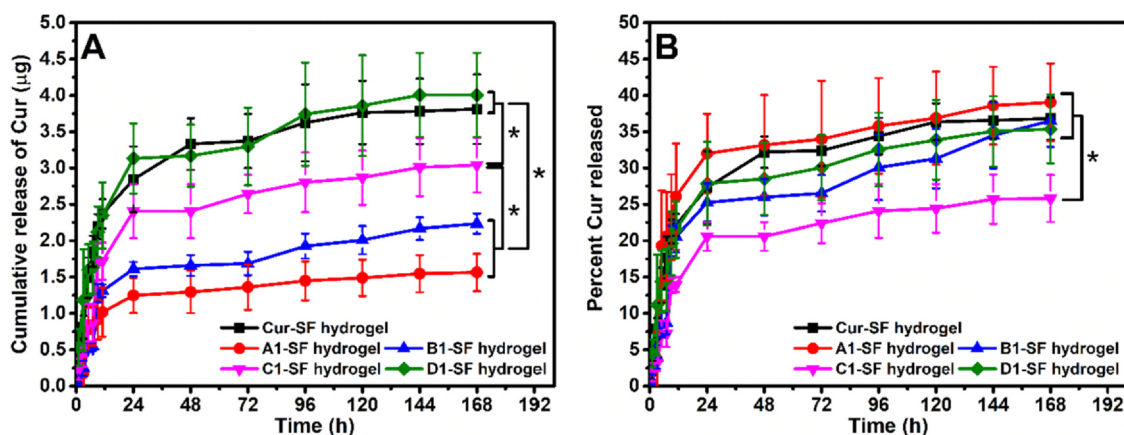


Fig. 8. Cur release from Cur-SF hydrogels and liposome (A1, B1, C1, D1)-induced SF hydrogels in PBS containing 10% FBS: (A) Cumulative amount of Cur released in 1 mL release media and (B) Percentage of Cur released at each time-point relative to the initial Cur content in hydrogels (* represented statistical difference at $p \leq 0.05$ of the release data at final time-point).

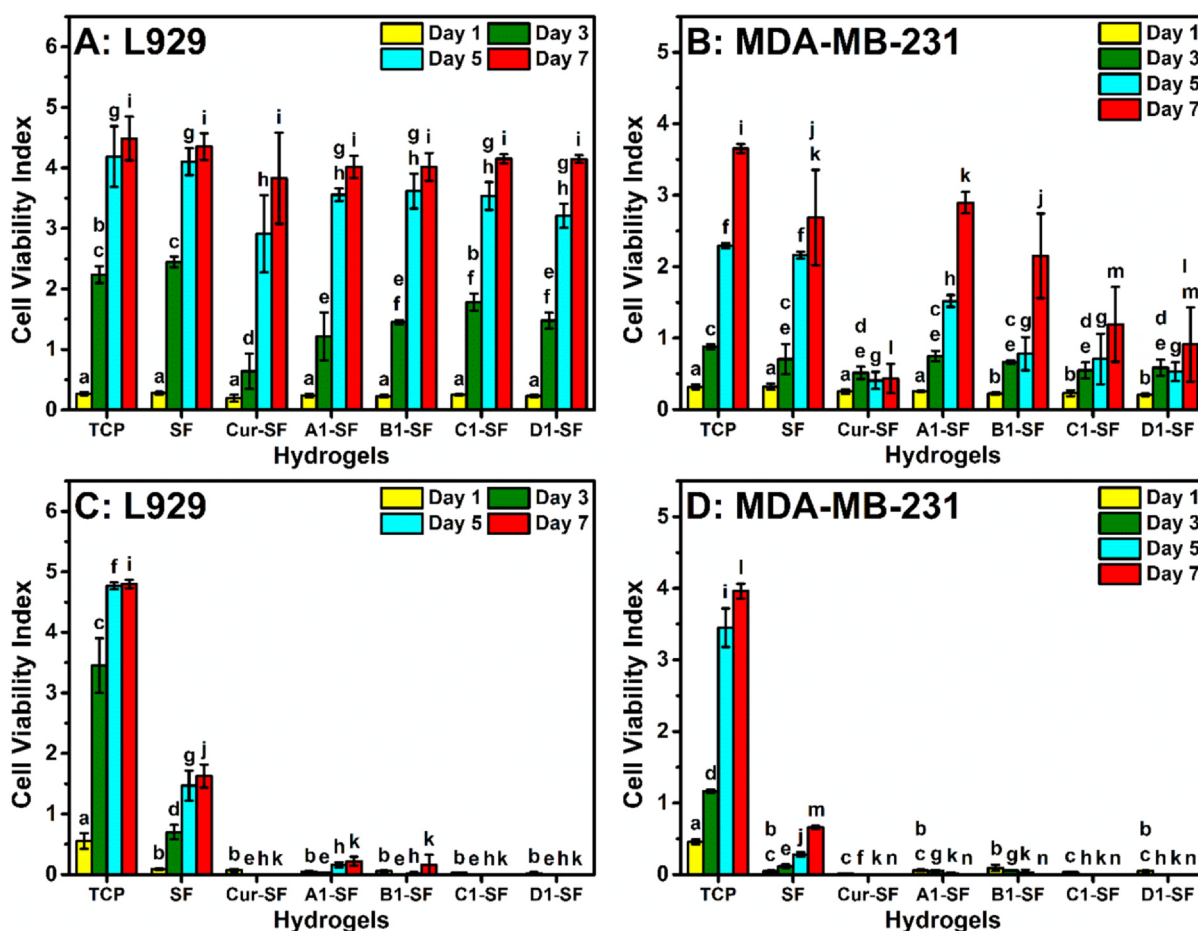


Fig. 9. Cell viability determined by WST-1 cell metabolic assay of (A) L929 and (B) MDA-MB-231 cultured on plate and exposed to the released Cur from immersed samples in culture media, and of (C) L929 and (D) MDA-MB-231 seeded on the hydrogel samples. TCP, SF and Cur-SF hydrogels were used as blank, negative, and positive control, respectively. Alphabetical notations indicated statistical difference at $p \leq 0.05$ compared between each sample within the same time point.

fluorescence staining images, respectively. Most cells in the TCP group and negative control (SF hydrogels) were negatively stained by both dyes, presenting the low intensity of annexin V and 7-AAD fluorescence dyes. Conversely, in Cur-SF and liposome-SF groups, the majority of cells visible in the bright field images were stained by annexin V and 7-AAD as well as an increasing of the fluorescence intensity of both dyes. Similar results were obtained for MDA-MB-231 (Fig. 10C and D), which

no stained cell was observed in TCP and SF groups. Cells exposed to the released components from A1, B1 and C1-SF hydrogels were stained with green and red dyes. Cells exposed to Cur displayed a high intensity ratio of annexin V to 7-AAD stains, which could indicate an early apoptosis of the cells.

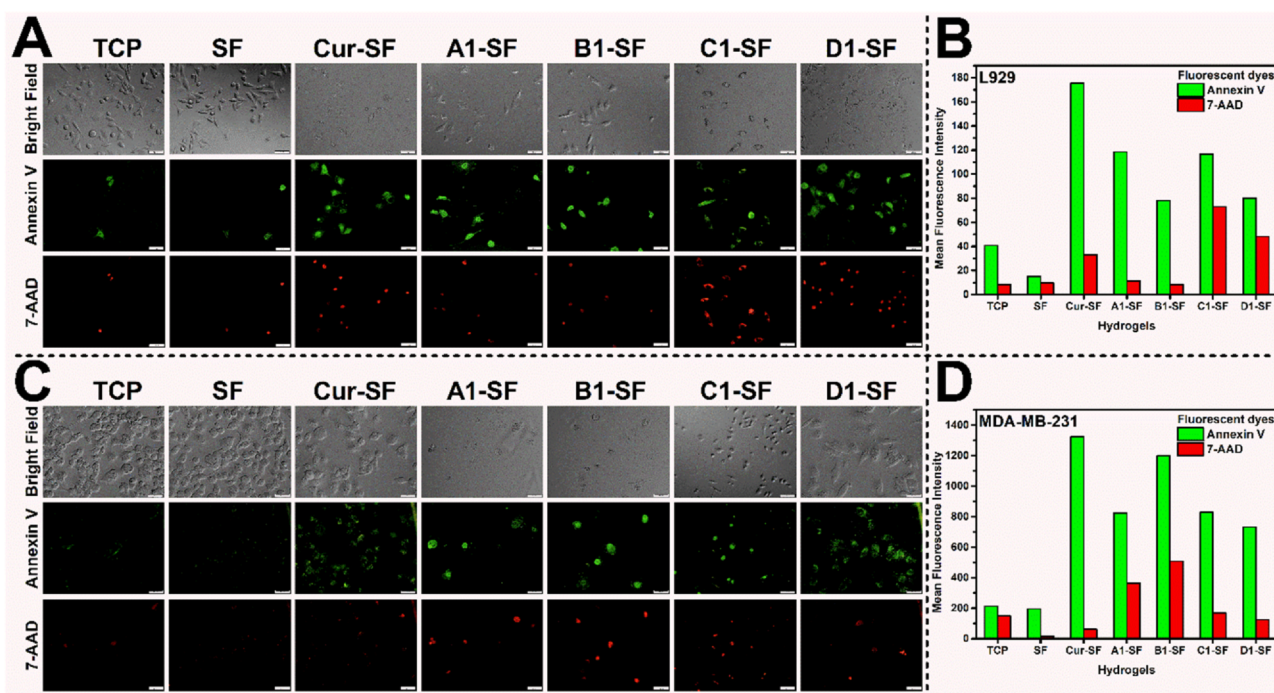


Fig. 10. Apoptosis staining of cells cultured on plates and exposed to the release Cur from hydrogels for 1 day: (A and C) Bright-field images and annexin V (green) and 7-AAD (red) fluorescent staining of L929 and MDA-MB-231, respectively (scale bar = 50 μ m) Positive staining of both dyes indicates cell death or late apoptosis, while single staining of annexin V indicates an early apoptosis. (B and D) Quantitative analysis of the fluorescence intensity of the stained L929 and MDA-MB-231 cells, respectively.

4. Discussion

In this work, DMPG-based liposomes were prepared to entrap a bioactive substance and to accelerate the gelation of SF, as reported in our previous study (Laomeephol et al., 2020). The addition of DMPG in the lipid mixtures for liposomes preparation has been performed to prevent aggregation, to reduce physical degradation of the vesicular structures (New, 1990), or to enhance electrostatic interactions with positively charged molecules (Were et al., 2003). Since there was no report on using liposomes prepared with DMPG to entrap Cur but only other lipophilic drugs (Han et al., 2002; Sampedro et al., 1994), the liposomes with different phospholipids (DMPG:DMPC) and cholesterol ratio were produced to evaluate the suitability of the liposome formulations for Cur loading. From Table 2, it can be observed that the liposome size was between 100 and 300 nm, except for A0 and B0 formulae, which their size distribution was highly scattered. From TEM images (Fig. 3), shape irregularity and vesicle aggregation can be observed in A1 and B1 liposomes, while a round morphology was noticed for the liposomes with 5:5 and 3:7 DMPG:DMPC ratios. This could indicate that the higher ratio of DMPG to DMPC resulted in a large size variation and aggregation. The size of liposomes with Chol was more controllable and stable. Indeed, Chol increases the stability of liposomes by its insertion into the lipid bilayers and enhancement of membrane integrity (Gregoriadis and Davis, 1979; New, 1990).

Approximately 50–100% EE was achieved (Table 2) depending on the ratio of DMPG:DMPC and the Chol content. The increase of DMPC-to-DMPG ratio resulted in a higher %EE. Even the addition of Chol was able to maintain liposomal structures as the results shown in Table 2 and Fig. 3, a higher Chol ratio led to a lower %EE. From molecular dynamic simulations, the position of Cur in the lipid bilayer is proposed at the center of lipid membranes, forming hydrogen bonds and hydrophobic interactions with the phospholipids (Jalili and Saeedi, 2016). It is possible that the location of Cur is in the same regions occupied by Chol (New, 1990), leading to a competitive localization. So, a greater amount of Chol could reduce the entrapment efficiency of Cur in lipid

bilayers.

As aforementioned, due to the lipophilic nature of Cur as well as its rapid degradation, Cur entrapment in liposomes can enhance the loading amount in aqueous environment and prevent hydrolysis. The results showed that the entrapment of Cur in liposomes drastically increased the amount (Fig. 4), from 0.54 μ g/mL curcuminoids obtained from direct dissolution of Cur powder in water to approximately 100–600 μ g/mL in the liposomes. The bioactive curcuminoids were preserved after storage at 4 $^{\circ}$ C for 2 weeks, comparing to about 90% loss of active Cur derivatives in the Cur aqueous solution. It can be confirmed that liposome formulations can enhance the amount and stability of lipophilic substances, such as Cur, by accommodating these molecules in the lipid bilayers. As a result, chemical degradations, such as photo-degradation or hydrolysis, are prevented (Mehanny et al., 2016). However, the 2-week stability studies of the liposomes as well as the bioactivities of the entrapped drugs could be too short for the practical uses. To enhance their stability, liposomes could be stored in the lyophilized form and reconstituted immediately before hydrogel preparation.

Without the physical intervention or chemical addition, the gelation time of regenerated SF solution is about several days or weeks depending on its concentration, temperature, pH and the presence of ions (Kim et al., 2004; Matsumoto et al., 2006). In our previous study, DMPG, a negative-charged phospholipid, was able to induce the gelation of SF within 10–40 min for DMPG concentrations ranging from 5 to 15 mM. Electrostatic and hydrophobic interactions were proposed for facilitating the self-assembly of SF. Therefore, in this work, 10 mg/mL liposomes, which is equivalent to 15 mM phospholipids, were mixed with 3% SF solution. Gel formation of SF occurred within 3 to 170 min. A faster gelation was noticed in this study due to the absence of salts since the ionic species can disturb electrostatic interactions between DMPG and SF chains. Noticeably, a higher ratio of DMPC resulted in a longer gelation time, which was in an agreement with our previous report (Laomeephol et al., 2020). The incorporation of Chol could increase the integrity of lipid bilayers, resulting in the extension of SF

gelation time. Mechanisms of gelation of DMPG-SF could result from the interaction of SF chains and the hydrophobic region of DMPG, which was corroborated by the TEM images (Fig. 6). Smaller vesicles of A1 (comparing to Fig. 3A) were noticed, which might result from SF chain insertion into the liposomal structures and subsequent vesicular breakage. Therefore, a higher Chol ratio probably increases the difficulty of SF chains to insert through lipid bilayers and interact with alkyl chain of phospholipids.

Elastic moduli of the Cur- and liposome-incorporated SF hydrogels were significantly lower than that of the regenerated SF gel. As previously discussed by Dubey et al. (2015), the incorporation of small molecules or particles could influence the mechanical stability of the materials. Furthermore, the SF hydrogels induced by the liposomes with higher DMPG ratio, namely A1-SF and B1-SF, displayed different mechanical properties. The elastic moduli of these hydrogels were lower than others, but the stress and strain at the yield point were higher. After the elastic limit, stress decreased over a range of strain, corresponding to a brittle material. It is possible that a high ratio of DMPG could result in more interactions between SF and DMPG, leading to the insertion of SF chains into the liposome vesicles. Furthermore, an interspersed of small vesicles, as seen in Fig. 6A, could interfere the chain-chain interactions of SF. Therefore, the materials could have a high tendency to lose their plasticity and to be unable to withstand the deformation when a high strain was applied.

The release of Cur from liposome-SF hydrogels showed a burst release in the first 24 h before subsequent gradual release (Fig. 8). Similar release profiles were obtained for the Cur-SF hydrogels. The direct entrapment of Cur in SF scaffolds allowed the controlled release of Cur from the SF, due to the binding of Cur with the hydrophobic regions of SF chains (Kasaju and Bora, 2012). Moreover, it is possible that the precipitated Cur, as noticed from the SEM image (Fig. 5), act as a reservoir for the slow release. Therefore, no difference of release pattern of Cur from Cur-SF hydrogels and liposome-include SF hydrogels was noticed. However, the advantage of Cur entrapment in the liposomes is the absence of organic solvents, namely DMSO, for Cur dissolution. Furthermore, the gelation of SF can occur by simply mixing the Cur liposomes with SF solution.

The role of Cur in the cancer treatment has been extensively investigated *in vitro* and *in vivo*. It has been shown that Cur inhibits the initiation and progression of tumors through the inhibition of cell overgrowth and the induction of cellular apoptosis (Shishodia et al., 2007). The effect of Cur in the growth inhibition of cancer cells, namely MDA-MB-231, was determined from the viability of cells cultured on plate against Cur released from the hydrogels (Fig. 9A and B). The results were compared to the fibroblastic cell line, L929. For MDA-MB-231, D1-SF hydrogels showed the lowest cell survival at 7 days, which was comparable to Cur-SF group. Moreover, the viability of cells against Cur from A1-SF and B1-SF hydrogels showed no significant differences with the SF group. The cell viability followed a similar trend to the results of Cur content analysis presented in Table 2. Apoptosis staining (Fig. 10) also showed the cell population undergoing apoptotic events after 1-day exposure to released Cur, confirming the activity of Cur in cell growth inhibition. Interestingly, the normal cell viability of L929 was noticed in all groups. There is a report demonstrating the cytotoxicity of Cur for L929 cells, of which the generation of reactive oxygen species led to an induction of cellular apoptosis in a dose-dependent manner (Thayyullathil et al., 2008). However, our results showed that the dose of released Cur did not deteriorate L929 proliferation since the metabolic activity at day 7 of all groups were comparable. At day 3, the cell viability was relatively low in Cur-SF and liposome-SF groups comparing to TCP and SF groups. The results were in accordance with the apoptosis staining (Fig. 10A), being the apoptotic cells after 1-day exposure to the released Cur. It is possible that Cur might affect the proliferation of L929, but the cells could recover and return to normal proliferation afterwards.

Cells cultured on SF hydrogels showed significantly low attachment

and proliferation comparing to their culture on TCP (Fig. 9C and D). These findings are in accordance with other studies (Acharya et al., 2008; Madden et al., 2011), since the absence of cell-adhesion motifs was reported for SF derived from mulberry silkworms (Zhou et al., 2001). This characteristic could synergize with the cytotoxicity of Cur, resulting in an extremely low viability of cells cultured on Cur-SF and liposome-SF hydrogels. These results support the application of the developed liposome-SF hydrogels as a filler after tumor resection. Indeed, the native properties of SF, which are unfavorably support the cell attachment but cytocompatible, together with the dose-dependent cytotoxicity of Cur, would be suitable to fill the space and to eradicate the leftover tumor cells after the tumor resection.

5. Conclusion

The liposomes composed of DMPG, DMPC and/or cholesterol possess a dual function as a delivery system of Cur and an inducer of SF hydrogel formation. Cur was successfully loaded in the liposomes with 50–100% EE, depending on the different formulations. Consequently, the amount and the stability of curcumin against photo degradation and hydrolysis were enhanced. The gelation of the SF solutions after mixing with liposomes occurred within 3 min to longer than 6 h, depending on the phospholipid composition and the presence of Chol. The effect of the Cur released from the hydrogels in the cell growth inhibition was observed only in the breast cancer cell line. However, together with the nature of SF hydrogel surfaces, the cells cultured on Cur-containing SF hydrogels exhibited very low cell viability. Therefore, the developed liposome-SF hydrogels could be used as potential delivery systems locally applied into a cavity after surgical resection of solid tumors, such as breast cancers.

CRediT authorship contribution statement

Chavee Laomeephol: Conceptualization, Methodology, Formal analysis, Investigation, Writing - original draft, Visualization. **Helena Ferreira:** Writing - review & editing. **Sorada Kanokpanont:** Writing - review & editing. **Nuno M. Neves:** Writing - review & editing. **Hisatoshi Kobayashi:** Conceptualization, Methodology, Validation, Resources, Supervision, Project administration, Funding acquisition. **Siriporn Damrongsakkul:** Conceptualization, Validation, Resources, Supervision, Project administration, Funding acquisition.

Declaration of Competing Interest

The authors declare that they have no known competing financial interests or personal relationships that could have appeared to influence the work reported in this paper.

Acknowledgements

An International Cooperative Graduate School (ICGS) Fellowship under the “Chulalongkorn University - NIMS Cooperative Graduate School Program” was acknowledged for supporting the exchange student to conduct the collaborative research project. The PhD grants for Chavee Laomeephol were supported by “The 100th Anniversary Chulalongkorn University Fund for Doctoral Scholarship” and “The 90th Anniversary Chulalongkorn University Fund (Ratchadaphiseksomphot Endowment Fund)”. TEM observation was kindly supported by NIMS microstructural characterization platform, and DLS and LC/MS measurements were supported by NIMS molecule & materials synthesis platform as a program of “Nanotechnology Platform” of the Ministry of Education, Culture, Sports, Science and Technology (MEXT), Japan.

References

- Acharya, C., Ghosh, S.K., Kundu, S.C., 2008. Silk fibroin protein from mulberry and non-mulberry silkworms: cytotoxicity, biocompatibility and kinetics of L929 murine fibroblast adhesion. *J. Mater. Sci. - Mater. Med.* 19, 2827–2836.
- Amornsudthiwat, P., Mongkolnavin, R., Kanokpanont, S., Panpranot, J., Wong, C.S., Damrongsakkul, S., 2013. Improvement of early cell adhesion on Thai silk fibroin surface by low energy plasma. *Colloids Surf., B* 111, 579–586.
- Bhattacharjee, P., Kundu, B., Naskar, D., Kim, H.-W., Maiti, T.K., Bhattacharya, D., Kundu, S.C., 2017. Silk scaffolds in bone tissue engineering: An overview. *Acta Biomater.* 63, 1–17.
- Ceelen, W., Pattyn, P., Mareel, M., 2014. Surgery, wound healing, and metastasis: Recent insights and clinical implications. *Crit. Rev. Oncol./Hematol.* 89, 16–26.
- Dubey, P., Nawale, L., Sarkar, D., Nisal, A., Prabhune, A., 2015. Sphorolipid assisted tunable and rapid gelation of silk fibroin to form porous biomedical scaffolds. *RSC Adv.* 5, 33955–33962.
- Gaillit, J., Clark, R.A.F., 1994. Wound repair in the context of extracellular matrix. *Curr. Opin. Cell Biol.* 6, 717–725.
- Gregoriadis, G., Davis, C., 1979. Stability of liposomes in vivo and in vitro is promoted by their cholesterol content and the presence of blood cells. *Biochem. Biophys. Res. Commun.* 89, 1287–1293.
- Grijalvo, S., Mayr, J., Eritja, R., Díaz, D.D., 2016. Biodegradable liposome-encapsulated hydrogels for biomedical applications: a marriage of convenience. *Biomater. Sci.* 4, 555–574.
- Han, I., Jun, M.S., Kim, M.K., Kim, J.C., Sohn, Y.S., 2002. Liposome Formulations for Effective Administration of Lipophilic Malonoplatinum(II) Complexes. *Jpn. J. Cancer Res.* 93, 1244–1249.
- Jalili, S., Saeedi, M., 2016. Study of curcumin behavior in two different lipid bilayer models of liposomal curcumin using molecular dynamics simulation. *J. Biomol. Struct. Dyn.* 34, 327–340.
- Kasoju, N., Bora, U., 2012. Fabrication and characterization of curcumin-releasing silk fibroin scaffold. *J. Biomed. Mater. Res. B Appl. Biomater.* 100B, 1854–1866.
- Kim, U.-J., Park, J., Li, C., Jin, H.-J., Valluzzi, R., Kaplan, D.L., 2004. Structure and Properties of Silk Hydrogels. *Biomacromolecules* 5, 786–792.
- Kundu, B., Rajkhowa, R., Kundu, S.C., Wang, X., 2013. Silk fibroin biomaterials for tissue regenerations. *Adv. Drug Deliv. Rev.* 65, 457–470.
- Laomeephol, C., Guedes, M., Ferreira, H., Reis, R.L., Kanokpanont, S., Damrongsakkul, S., Neves, N.M., 2020. Phospholipid-induced silk fibroin hydrogels and their potential as cell carriers for tissue regeneration. *J. Tissue Eng. Regen. Med.* 14, 160–172.
- Li, J., Wang, X., Zhang, T., Wang, C., Huang, Z., Luo, X., Deng, Y., 2015. A review on phospholipids and their main applications in drug delivery systems. *Asian J. Pharm. Sci.* 10, 81–98.
- Madden, P.W., Lai, J.N.X., George, K.A., Giovenco, T., Harkin, D.G., Chirila, T.V., 2011. Human corneal endothelial cell growth on a silk fibroin membrane. *Biomaterials* 32, 4076–4084.
- Matsumoto, A., Chen, J., Collette, A.L., Kim, U.-J., Altman, G.H., Cebe, P., Kaplan, D.L., 2006. Mechanisms of Silk Fibroin Sol–Gel Transitions. *J. Phys. Chem. B* 110, 21630–21638.
- Mehanny, M., Hathout, R.M., Geneidi, A.S., Mansour, S., 2016. Exploring the use of nanocarrier systems to deliver the magical molecule; Curcumin and its derivatives. *J. Control. Release* 225, 1–30.
- New, R.R.C., 1990. *Liposomes: a practical approach*. Oxford University Press, New York.
- Patra, J.K., Das, G., Fraceto, L.F., Campos, E.V.R., Rodriguez-Torres, M.D.P., Acosta-Torres, L.S., Diaz-Torres, L.A., Grillo, R., Swamy, M.K., Sharma, S., Habtemariam, S., Shin, H.-S., 2018. Nano based drug delivery systems: recent developments and future prospects. *J. Nanobiotechnol.* 16, 71.
- Pitorre, M., Gondé, H., Haury, C., Messous, M., Poilane, J., Boudaud, D., Kanber, E., Rossemond Ndombina, G.A., Benoit, J.-P., Bastiat, G., 2017. Recent advances in nanocarrier-loaded gels: Which drug delivery technologies against which diseases? *J. Control. Release* 266, 140–155.
- Qi, Y., Min, H., Mujeeb, A., Zhang, Y., Han, X., Zhao, X., Anderson, G.J., Zhao, Y., Nie, G., 2018. Injectable Hexapeptide Hydrogel for Localized Chemotherapy Prevents Breast Cancer Recurrence. *ACS Appl. Mater. Interfaces* 10, 6972–6981.
- Ramalingam, P., Ko, Y.T., 2014. A validated LC-MS/MS method for quantitative analysis of curcumin in mouse plasma and brain tissue and its application in pharmacokinetic and brain distribution studies. *J. Chromatogr. B* 969, 101–108.
- Sampedro, F., Partika, J., Santalo, P., Molins-Pujol, A.M., Bonal, J., Perez-Soler, R., 1994. Liposomes as carriers of different new lipophilic antitumour drugs: A preliminary report. *J. Microencapsul.* 11, 309–318.
- Shishodia, S., Chaturvedi, M.M., Aggarwal, B.B., 2007. Role of Curcumin in Cancer Therapy. *Curr. Probl. Cancer* 31, 243–305.
- Talebian, S., Foroughi, J., Wade, S.J., Vine, K.L., Dolatshahi-Pirouz, A., Mehrali, M., Conde, J., Wallace, G.G., 2018. Biopolymers for Antitumor Implantable Drug Delivery Systems: Recent Advances and Future Outlook. *Adv. Mater.* 30, 1706665.
- Thayyullathil, F., Chathoth, S., Hago, A., Patel, M., Galadari, S., 2008. Rapid reactive oxygen species (ROS) generation induced by curcumin leads to caspase-dependent and -independent apoptosis in L929 cells. *Free Radical Biol. Med.* 45, 1403–1412.
- Vachiraroj, N., Ratanavaraporn, J., Damrongsakkul, S., Pichyangkura, R., Banaprasert, T., Kanokpanont, S., 2009. A comparison of Thai silk fibroin-based and chitosan-based materials on in vitro biocompatibility for bone substitutes. *Int. J. Biol. Macromol.* 45, 470–477.
- Wang, X., Kluge, J.A., Leisk, G.G., Kaplan, D.L., 2008. Sonication-induced gelation of silk fibroin for cell encapsulation. *Biomaterials* 29, 1054–1064.
- Wang, Y.-J., Pan, M.-H., Cheng, A.-L., Lin, L.-L., Ho, Y.-S., Hsieh, C.-Y., Lin, J.-K., 1997. Stability of curcumin in buffer solutions and characterization of its degradation products. *J. Pharm. Biomed. Anal.* 15, 1867–1876.
- Were, L.M., Bruce, B.D., Davidson, P.M., Weiss, J., 2003. Size, Stability, and Entrapment Efficiency of Phospholipid Nanocapsules Containing Polypeptide Antimicrobials. *J. Agric. Food. Chem.* 51, 8073–8079.
- William, J.G., Benjamin, O.A., Ron, B., Sarah, L.B., Harold, J.B., Amy, C., Anthony, D.E., William, B.F., Andres, F., Sharon, H.G., Matthew, P.G., Lori, J.G., Steven, J.I., Janice, L., Marcom, P.K., Ingrid, A.M., Beryl, M., Meena, S.M., Ruth, M.O.R., Sameer, A.P., Lori, J.P., Elizabeth, C.R., Kilian, E.S., Lee, S.S., Amy, S., Karen Lisa, S., Mary Lou, S., Hatem, S., George, S., Melinda, L.T., John, H.W., Rashmi, K., Dorothy, A.S., 2018. Breast Cancer, Version 4.2017, NCCN Clinical Practice Guidelines in Oncology. *J. Natl. Compr. Canc. Netw.* 16, 310–320.
- Wolinsky, J.B., Colson, Y.L., Grinstaff, M.W., 2012. Local drug delivery strategies for cancer treatment: gels, nanoparticles, polymeric films, rods, and wafers. *J. Control Release* 159, 14–26.
- Yang, K.-Y., Lin, L.-C., Tseng, T.-Y., Wang, S.-C., Tsai, T.-H., 2007. Oral bioavailability of curcumin in rat and the herbal analysis from *Curcuma longa* by LC-MS/MS. *J. Chromatogr. B* 853, 183–189.
- Yucel, T., Lovett, M.L., Kaplan, D.L., 2014. Silk-based biomaterials for sustained drug delivery. *J. Control Release* 190, 381–397.
- Zhou, C.-Z., Confalonieri, F., Jacquet, M., Perasso, R., Li, Z.-G., Janin, J., 2001. Silk fibroin: Structural implications of a remarkable amino acid sequence. *Prot.: Struct. Funct., Bioinform.* 44, 119–122.